15

# Testing natural and synthetic micas as detectors of accelerated heavy ions

© E.V. Andreev,[1] P.Y. Apel,[1,2] T.M. Bublikova,[3] I.I. Zasavitskiy,[2] N.S. Konovalova,[2] N.M. Okateva,[2] N.G. Polukhina,[2] T.V. Setkova,[3] N.I. Starkov,[2] E.N. Starkova,[2] M.M. Chernyavskiy,[2] T.V. Shchedrina[2]

[1] Joint Institute for Nuclear Research,
141980 Dubna, Moscow oblast, Russia
[2] Lebedev Physical Institute, Russian Academy of Sciences,
119991 Moscow, Russia
[3] Institute of Experimental Mineralogy, Russian Academy of Sciences,
142432 Chernogolovka, Moscow region, Russia
e-mail: starkovaen@lebedev.ru

*Received May 6, 2025*
*Revised September 5, 2025*
*Accepted September 26, 2025*

In the Laboratory of Elementary Particles of the LPI the dielectric materials are being tested as detectors of fission fragments of superheavy nuclei in the thermochromatographic column of the JINR Superheavy Elements Factory. In the paper, the results of testing various micas irradiated with accelerated Xe and Bi ions with energies from 83 to 670 MeV are analyzed. It is shown that two types of natural mica retain ion tracks when heated after irradiation up to 300 °C and 500 °C, which means their fundamental applicability in experiments studying the properties of superheavy nuclei.

**Keywords:** micas for of heavy ion registration, annealing at high temperatures, image processing on an automated microscope.

DOI: 10.61011/TP.2026.01.62856.106-25

## Introduction

A problem of synthesis of superheavy elements is directly related to an issue of their registration. The Laboratory of Elementary Particles of the Lebedev Physical Institute (LEP LPI) studies usability of various dielectrics as materials for heavy nuclei detectors that can retain tracks when heated. Under conditions of a thermochromatographic column, products of disintegration of nuclei with an atomic number exceeding 112 are registered at high temperatures that can be up to 500 °C. In these conditions, silicon and emulsion detectors can not be used for registering the disintegration products, and a detector material can be dielectrics, in particular, glasses and micas.

The Laboratory of Elementary Particles of the Lebedev Physical Institute (LEP LPI) studies usability of various dielectrics as materials for heavy nuclei detectors that can retain tracks when heated. Under high-temperature conditions the tracks can be annealed (fully or partially annihilated) in the dielectric detector, wherein an annealing degree primarily depends on the temperature and thermal effect duration.

The authors have performed a series of studies for investigating registration properties of glasses of various composition in different temperature conditions of irradiation and treatment [3–7]. According to the obtained results, at high temperatures, some glasses exhibit changes of the registration properties, which limit their usability in the proposed terms. For example,, the phosphate glass of the grade KFNS-3 and the quartz glass of the grade KU-2 can retain ion tracks, but under high-temperature conditions geometrical parameters of the track change, thereby making it difficult to identify the ions.

For heavy-ion detectors, experimental nuclear physics widely applies natural minerals and their synthetic analogues, in particular, micas (see, for example, [8–11]). The present study provides results of investigating several micas that are irradiated in an ion beam of a resonance cyclotron U-400 of the FLNR JINR and treated in various temperature modes. Usability of these materials as the heavy-ion detectors under conditions of the thermochromatographic column was analyzed.

## 1. Test samples

### 1.1. Chemical composition of the studied micas

One of the precious properties of micas is their high chemical stability. Besides, many micas are characterized by optical transparence and higher resistance to elevated temperatures than that for glasses. These factors have determined interest to the micas in these studies. Samples of four different micas, whose chemical composition is shown in the Table (where $n$ is a number of performed analyses, $\sigma$ is a mean-square error) have been tested: muscovite Ms, muscovite-lepidolite Ms-Lpd, the so-called „Indian“ muscovite Ms-In (the name is derived from an extraction deposit in the Bihar mica-producing region, India [12])

Chemical composition of the tested micas (mass%)

| Component, % | Muscovite-lepidolite Ms-Lpd | | „Indian“ muscovite Ms-In | | Mica Ms | | Fluorophlogopite SM-310 |
|---|---|---|---|---|---|---|---|
| | $n = 9$ | $2\sigma$ | $n = 9$ | $2\sigma$ | $n = 14$ | $2\sigma$ | |
| $SiO_2$ | 42.5 | 0.5 | 44.1 | 0.5 | 46.3 | 0.5 | 39.0 – 43.0 |
| $TiO_2$ | 0.0 | 0.0 | 0.6 | 0.2 | 0.3 | 0.2 | 0.0 |
| $Al_2O_3$ | 32.1 | 0.5 | 33.8 | 0.5 | 33.4 | 0.5 | 9.0 – 12.0 |
| FeO | 2.2 | 0.3 | 1.3 | 0.3 | 1.8 | 0.3 | 0.0 |
| MnO | 0.5 | 0.2 | 0.0 | 0.0 | 0.0 | 0.2 | 0.0 |
| MgO | 0.0 | 0.0 | 0.7 | 0.2 | 1.0 | 0.2 | 27.0 – 30.0 |
| $K_2O$ | 9.9 | 0.4 | 10.5 | 0.4 | 10.8 | 0.4 | 7.0 – 9.0 |
| $Na_2O$ | 0.7 | 0.3 | 0.8 | 0.2 | 0.8 | 0.2 | 0.0 |
| F | 3.3 | 0.9 | 0.0 | 0.0 | 0.0 | 0.0 | 9.0 – 12.0 |
| $Li_2O_{cal}$ | 3.4 | – | – | – | – | – | – |
| $H_2O_{cal.}$ | 2.4 | – | 4.3 | – | 4.5 | – | – |
| In total | 97.1 | | 96.0 | | 98.8 | | 100.0 |

and a synthetic mica fluorophlogopite CM-310 produced by NPO „Luch“.

The chemical composition of the natural micas Ms-Lpd, Ms-In and Ms was determined as part of the present study using electron-probe X-ray spectrum analysis on a digital scanning microscope Tescan Vega II XMU with an energy-dispersive spectrometer INCA Energy 450 equipped with a semiconductor Si(Li) detector INCA x-sight and a wave-dispersion spectrometer INCA Wave 700 in Institute of Experimental Mineralogy RAS. The measurements were performed at an accelerating voltage of 20 kV. Zonality of element distribution in the samples was found by scanning over areas of the size $65 \times 65\,\mu$m, which made it possible to obtain detailed information about the variations in chemical composition. In order to provide for a conductive layer necessary for analysis, a carbon film of the thickness of 15 nm was applied to the samples before shooting. The electron-probe X-ray spectrum analysis does not allow to determine the presence of lithium and hydrogen. In this regard, the content of $Li_2O$ and $H_2O$ in the samples was found based on calculating formula units per $22(-)$ charges by a difference.

The exact composition of fluorophlogopite of the grade SM-310 is a commercial information of the producer and is given in the form of ranges of contents of the basic elements.

### 1.2. Experimental conditions

The chemical composition of the muscovite-lepidolite (Ms-Lpd) mica is characterized by a high content of fluorine and a low content of iron and magnesium.Ms-Lpd is a low-iron lithium-aluminum mica forming a muscovite-lepidolite series of solid solutions. Muscovite ($KAl_2(Si_3Al)O_{10}(OH)_2$) is hardly melted and is resistant to acids: a hydrochloric acid almost makes no decomposition of it even when heated up to 300 °C, a sulfuric acid affects only while long heating. Lepidolite is less refractory than muscovite and it difficulty dissolves in acids only after melting. The thickness of the separable layers of Ms-Lpd is $50\,\mu$m. Its transparency degree makes it possible to view samples formed by two plates of the mineral on an optical microscope.

„Indian“ muscovite Ms-In is characterized by uniform distribution of the elements over the entire sample. The mineral has high structure perfection. The layers fit tightly, thereby preventing penetration of an etching solution into the sample.

The chemical composition of the Ms mica corresponds to the composition of the muscovite mineral, and by its composition and the element content the mineral is similar to the Ms-In mica. The distribution of the elements is uniform over the entire sample. The mineral layers have a thickness of $\sim 40\,\mu$m and, as in case of the Ms-In mica, fit together more tightly than those of Ms-Lpd, without separation from each other. While etching, the chemical solution does not penetrate deep into the sample, making it only slightly delaminated at the edges. The area of the tested mica samples made from 1 to 5 $cm^2$.

The material of fluorophlogopite (the ideal formula): $KMg_3(AlSi_3O_{10})F_2$) is a synthetic analogue of a natural phlogopite mica, exceeding it in thermal resistance. Several test samples of the size $3 \times 5 \times 10$ mm were manufactured for these studies as a part of scientific-technical cooperation of the authors with NPO „Luch“. Fluorophlogopite of the

grade SM-310 is an easily-treatable strong ceramic of high insulation properties.

In some cases, to obtain lower ion energies, a polyethylene terephtalate (PETP) film of the thickness of $7\,\mu$m was added to the particle path. As a result, energy of the ions incident on the sample surface at the angle of 45° made $\sim 83$ MeV (according to the calculations by the SRIM10 software [14]). Totally, in these studies 6 mica samples were irradiated with Xe ions of energy of 83 MeV and 6 samples were irradiated with Xe ions of energy of 160 MeV; 12 samples were irradiated with Bi ions of energy of 670 MeV; 4 fluorophlogopite samples SM-310 were irradiated with Xe ions of energy of 160 MeV.

Radiation-induced damage by charged particles in the dielectric was visualized by means of chemical etching. The irradiated samples of the natural micas were etched in a 40 % solution of fluoric acid HF in time increments from 5 to 15 min, and the fluorophlogopite samples were etched in 2.5 % HF and in 10 % NaOH. The etched channels formed by accelerated ions penetrating into the detector material were measured with $40^{\times}$ magnification on an optical microscope of the automated measuring complex PAVICOM in LEP LPI [15].

Results of the similar studies for various glasses are given in the paper [7]. In handling the glasses, when determining the length of the etched track, the thickness of the etched layer [16] was taken into account. The composition of the natural micas includes a large percentage of aluminum, thereby providing these minerals with high chemical stability. As a result, rates of their etching with fluoric acid range from 0.3 to $0.5\,\mu$m/h. Thus, for one hour of etching the thickness of the etched-off layer does not exceed $0.5\,\mu$m, which is almost by an order smaller than than the ame indicator for the glasses. Since the length of the etched tracks exceeds $10\,\mu$m, the thickness of the etched-off layer can be neglected when determining track lengths in the natural micas.

The maximum track length in this experiment is $\sim 35\,\mu$m; at a beam angle of 45°, such tracks penetrate into the mineral to a depth of $\sim 25\,\mu$m. Using a software embedded in the measuring complex PAVICOM, images of etched channels shaped like an ellipse were extracted under a microscope, and their length (major axis of the ellipse) and width (minor axis of the ellipse) were determined. The microscope focus depth under $40^{\times}$ magnification is $\sim 20-22\,\mu$m, and in a focused image of the track beginning its end is usually somewhat smeared in the view field of the microscope. The authors' software program of selecting images of individual tracks includes a contrast enhancement procedure, in which the smeared end of the track is also included into a unified cluster (a track projection image formed as a result of computer processing). As a result, the cluster length completely correspond to the projection of the etched channel, which makes it possible to determine the full length of the etched track with high accuracy.

An important characteristic that enables to determine the ion charge is a magnitude of its path in the detector material. Since the sample size significantly exceeds the length of the path of accelerated ions to a stop in the material, the stopping point of the ions is almost always located within the sample volume. As a result, an inflection point corresponding to ion stop in the detector material can be identified on a graph of an experimental dependence of the track projection length on the etching time. A steeper section at the beginning of the etching corresponds to an area of the material damage by the ion (the track area) with a higher etching rate as compared to the main material etching rate. After the inflection point, an undamaged material is being etched at a smaller rate [17,18]. Using this pattern, one can determine the value of the ion path in the mineral.

After irradiation, some samples were heated at 300 °C and 500 °C in a JINR muffle furnace with subsequent holding for 10 min and 3 h at these temperatures in order to estimate the track annealing degree. The results of the study of irradiated samples of four different micas with and without heating are presented below.

## 2. Results

### 2.1. Unheated testing

One sample of the Ms-Lpd mica was irradiated with the Xe ion beam with an energy of 160 MeV being transmitted through the PETP layer. One should note that mica processing has specific features differing it from the similar procedure for glass. Thus, when the Ms-Lpd samples are being degreased and etched, bubbles form between the mica layers due to penetration of liquid (Fig. 1, *a*), which however does not prevent the etched tracks from observation under the microscope. The ion tracks have been clearly visible starting from 20 min etching.

On Fig. 2, where a dependence of the track projection length on a plane of the Ms-Lpd sample on the etching time is presented, at the value of 100 min, a kink is observed, after which the curve has a less steep slope, indicating that the ion has reached a stopping point in the detector material [6]. The track projection length in this point is $(9 \pm 1)\,\mu$m. Taking into account the angle of incidence, the experimentally obtained ion path length in the mineral $L_{path} = (13 \pm 1)\,\mu$m and, consequently, the etching rate of the material in the track area is $(8 \pm 1)\,\mu$m/h. The path of Xe ions with an energy of 83 MeV, obtained using the SRIM10 program, is $11.5\,\mu$m, which is consistent with the experimental value obtained within the measurement errors.

The second sample of the Ms-Lpd mica was irradiated at an angle of 45° with Bi ions with an energy of 670 MeV. Fig. 3 shows photos of the sample irradiated surface at the different duration of etching.

In this case, the kink of the experimental curve that is a dependence of the track projection length on the sample plane on the etching time is observed at 40 min (Fig. 4). At this, the track projection length reaches $(22 \pm 1)\,\mu$m,

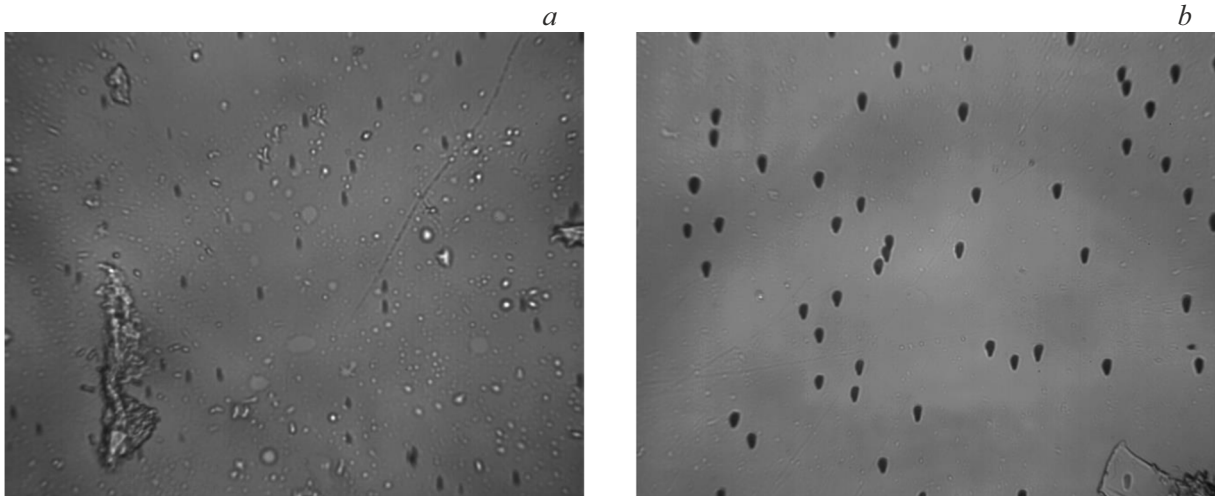



**Figure 1.** Photos of the tracks of Xe ions with an energy of 83 MeV obtained in the sample of the Ms-Lpd mica after etching in 40 % HF for 20 ($a$) and 80 ($b$) min. Frame size is $220 \times 280\,\mu$m, magnification is $40^{\times}$.

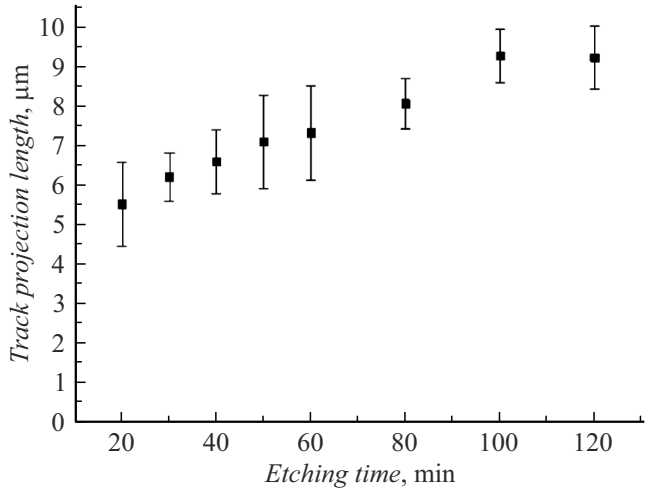



**Figure 2.** Dependence of the projection length of the tracks of Xe ions with an energy of 83 MeV on the surface of the Ms-Lpd mica sample on the etching time.

which corresponds to the path length $L_{path} = (31 \pm 1)\,\mu$m and the track etching rate $(47 \pm 1)\,\mu$m/h. The range of these ions, calculated by the SRIM10 software, makes 32.3 $\mu$m. $32.3\,\mu$m.

The first batch of the Ms-In mica samples was irradiated with Xe ions with an energy of 160 MeV at an angle of 45°. The tracks appeared after the first 10 min of etching; in 70 min of etching the track lengths noticeably increased (Fig. 5).

The inflection point of the experimental curve is observed at the 80th minute of etching (Fig. 6); the track projection length in this point is $(13 \pm 1)\,\mu$m, the path length is $L_{path} = (18 \pm 1)\,\mu$m ((an estimated path length is $17.3\,\mu$m), and the etching rate in the track area is $(13 \pm 1)\,\mu$m/h.

The second batch of the Ms-In mica samples was irradiated with Xe ions with an energy of 670 MeV at an angle of 45° (Fig. 7). The inflection point of the experimental dependence (Fig. 8) appears after the 45 minute etching, when the track projection length is $(21 \pm 1)\,\mu$m, which corresponds to the path length $L_{path} = (31 \pm 1)\,\mu$m (an estimated path length is $32.3\,\mu$m), and the etching rate in the track area is $(41 \pm 1)\,\mu$m/h.

One batch of the samples of the Ms mica was irradiated with a beam of the Xe ions with an energy of 160 MeV, which passed through the $7\,\mu$m PETP, as a result of which the energy of ions incident on the sample at an angle of 45° was 83 MeV. The tracks that appeared after the first 20 minutes of etching in 40 % HF turned out to be shorter than in the micas Ms-Lpd and Ms-In. Fig. 9 shows images of the tracks, while Fig. 10 shows a dependence of the length of the track projection on the sample surface on the etching time. The kink in the sequence of points occurs at the 80 minute of etching, wherein the track projection length is $(9 \pm 1)\,\mu$m, which corresponds to the path length $L_{path} = (14 \pm 1)\,\mu$m (an estimated path length is $11.5\,\mu$m), and the etching rate in the track area is $7 \pm 1)\,\mu$m/h.

The second batch of the Ms mica samples was irradiated with the Bi ion beam with an energy of 670 MeV. At an energy of 670 MeV, the Bi ion path in the Ms mica is $\sim 35\,\mu$m. According to an estimate obtained by means of the SRIM10 software, the ion transmitted through the $30\,\mu$m thick Ms sample leaves it with an energy of $\sim 45$ MeV. It results in etching at both sides of the sample. The thickness and transparency of the sample make the tracks visible under the microscope at both the sides (Fig. 11). In this case, the inflection point of the function is not observed (Fig. 12), and since the projection length of the Bi ion tracks $\sim 20 - 22\,\mu$m is achieved in the first 10 minutes of etching, one can obtain only an estimate of the lower boundary of the etching rate, which is $70 - 90\,\mu$m/h.

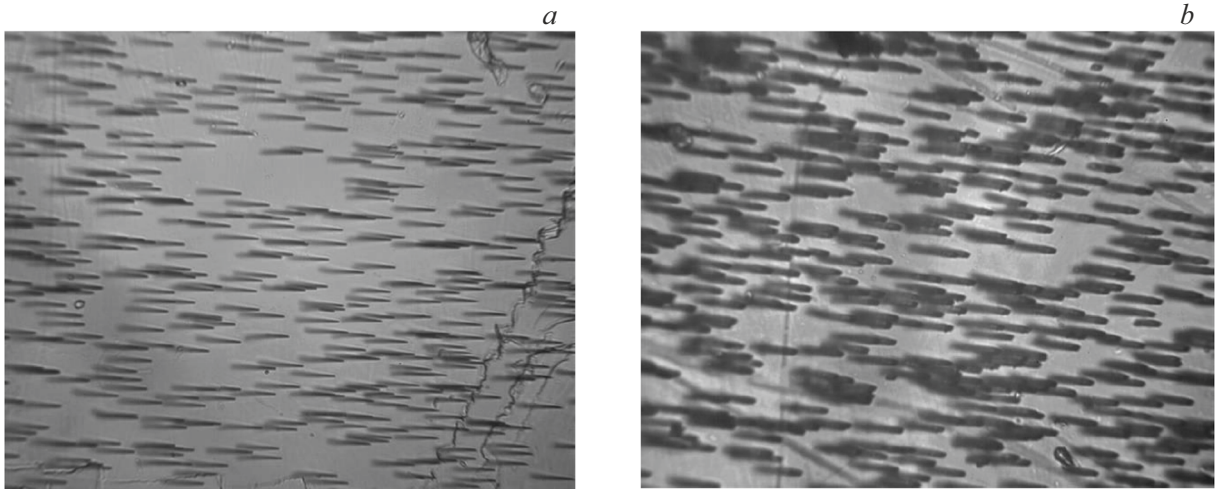



**Figure 3.** Photos of the tracks of Bi ions with an energy of 670 MeV in the Ms-Lpd mica sample after etching in 40 % HF for 20 ($a$) and 70 ($b$) min. The frame size is $220 \times 280\,\mu$m.

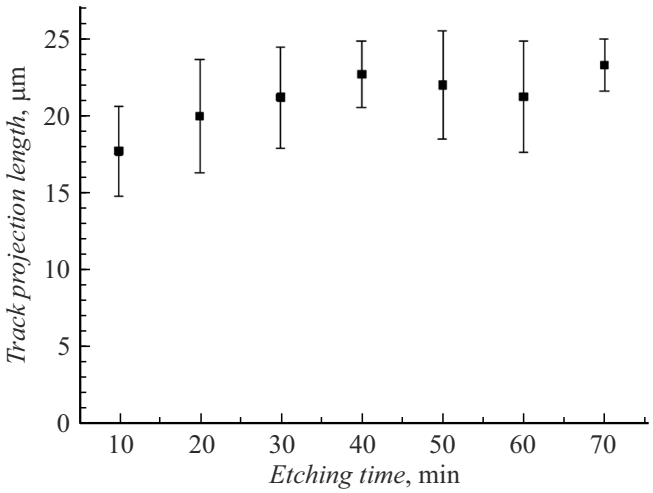



**Figure 4.** Dependence of the projection length of the tracks of Bi ions with an energy of 670 MeV on the surface of the Ms-Lpd mica sample on the etching time.

In a context of the set problem, the synthetic mica fluorophlogopite exhibits some technological drawbacks (Fig. 13). The irradiated samples of fluorophlogopite were etched with fluoric acid (2.5 % in volume by a pattern $20 \times 30 \times 40$ min) and with solution of sodium hydroxide 10 % NaOH. When etched in 2.5 % HF, the weight loss of the samples was 20 times higher than the one of the phosphate glasses etched in 20 % HF [5]. After each etching stage, the sample surface got looser and less transparent. On the contrary, when etching in 10 % NaOH, the weigh losses were not detected and the surface structure did not change, which meant no interaction of the material with an alkaline solvent. These results indicate the impossibility of using fluoroflogopite of the grade SM-310 to solve the tasks.

### 2.2. Testing when heating up to 300 °C

After being irradiated with Bi ions with an energy of 670 MeV, some of the Ms mica samples were annealed at the temperature of 300 °C with exposure at this temperature for 10 min. After annealing, visible tracks appeared in 50 min of etching in 40 % HF. The tracks turned out to be heavily annealed (Fig. 14, $a$, $b$), the track depth after temperature treatment of the sample did not exceed $8 - 10\,\mu$m. At the depth of $15\,\mu$m, the tracks were very short and were accompanied by a diffraction pattern, possibly, from a thin part of the track, which was not visible in the optical microscope (the effect of „healing“ of defects induced by the passage of the ions). On the back of the sample, the tracks were even paler and significantly shorter (Fig. 14, $c$), which can be related to reduction of ion energy as a result of transmission through the sample. Thus, it was shown by results of testing the Ms mica at a temperature of 300 °C that this mineral was very sensitive to annealing and could not be used under high-temperature conditions.

### 2.3. Testing at heating up to 500 °C

After irradiation at the angle of 45° with Bi ions with an energy of 670 MeV, the two samples of Ms-Lpd were heated to 500 °C with exposure of the first sample for 10 min and the second one for 3 h at this temperature. Fig. 15 shows images of the tracks obtained as a result of etching the annealed samples. An experimental dependence of the track projection length on the sample surface on the etching time is shown in Fig. 16. After annealing for 10 min, an inflection of the experimental curve is observed at the 25th minute of etching (Fig. 16, $a$), and at the 20th minute of etching (Fig. 16, $b$) after annealing for 3 h. The track projection length in the inflections points is $(19 \pm 2)\,\mu$m and $(19 \pm 2)\,\mu$m, while the full track length before the stop is $(28 \pm 2)\,\mu$m and $(27 \pm 2)\,\mu$m, respectively. The estimated

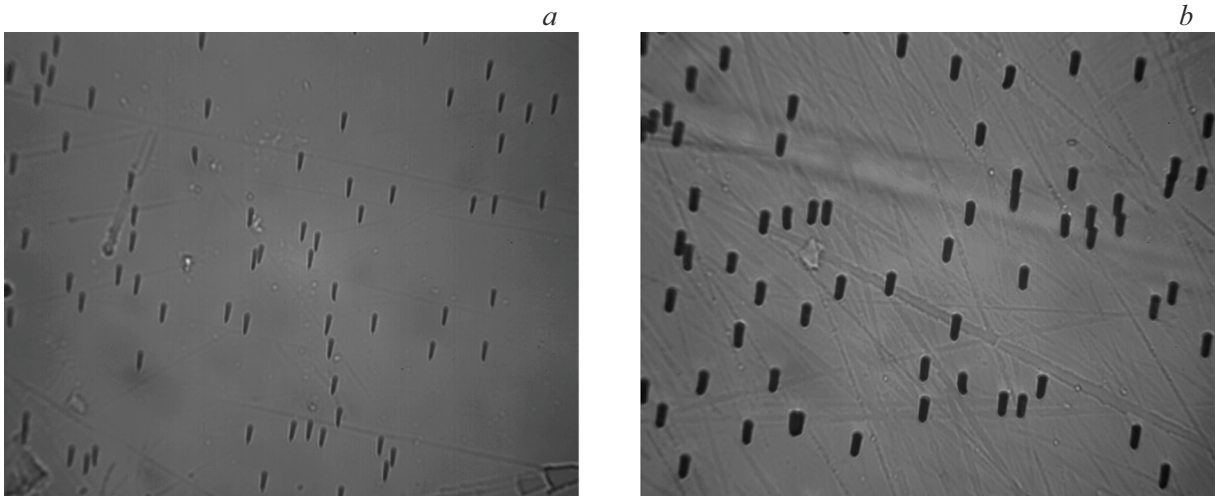



**Figure 5.** Photos of the tracks of Xe ions with an energy of 160 MeV obtained in the sample of the Ms-In mica after etching in 40 % HF for 20 ($a$) and 70 ($b$) min. The frame size is 220 × 280 $\mu$m.

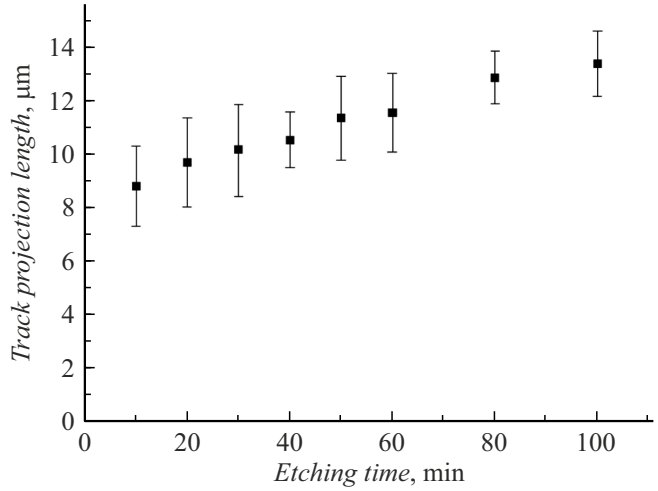



**Figure 6.** Dependence of the projection length of Xe ion tracks with an energy of 160 MeV on the surface of the Ms-In mica sample on etching time.

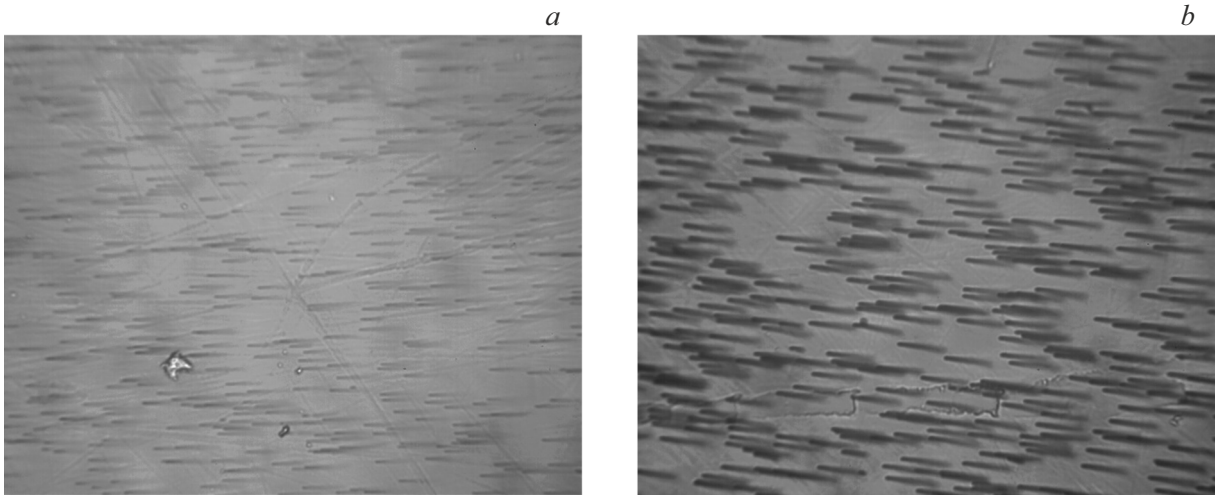



**Figure 7.** Photos of the Bi ion tracks with an energy of 670 MeV obtained in the Ms-In mica sample after etching in 40 % HF for 20 ($a$) and 60 ($b$) min. The frame size is 220 × 280 $\mu$m.

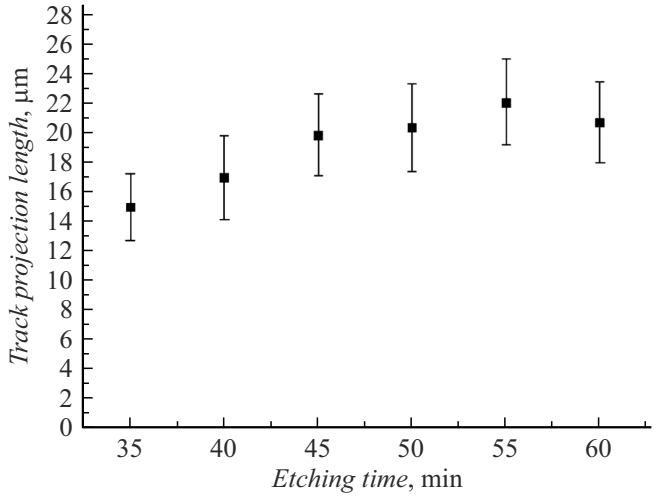



**Figure 8.** Dependence of the projection length of Bi ion tracks with an energy of 670 MeV on the surface of a mica sample Ms-In on the etching time.

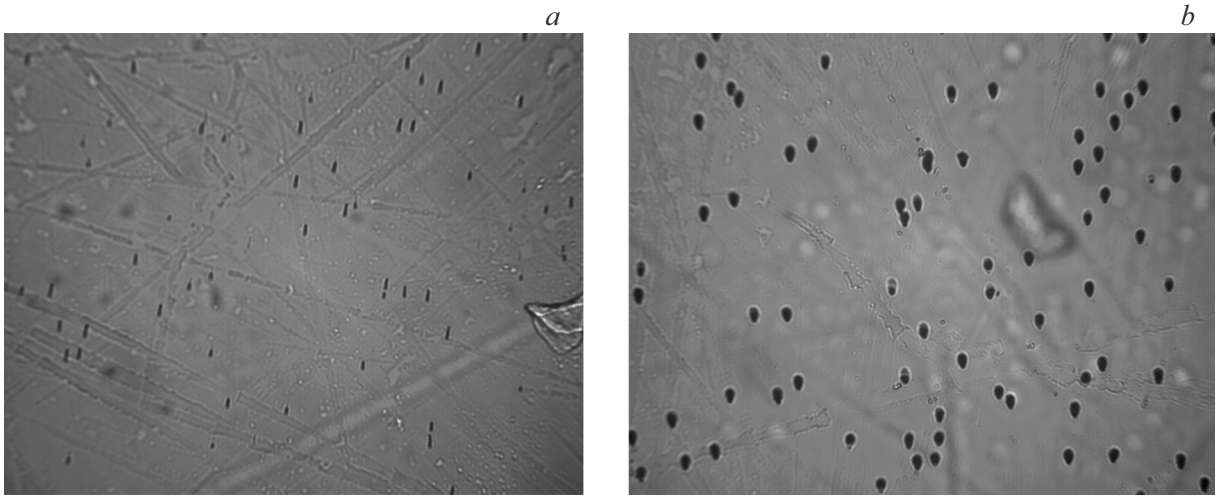



**Figure 9.** Photos of tracks of Xe ions with an energy of 83 MeV, which are obtained in the sample of the Ms mica after etching in 40 % HF for 20 ($a$) and 80 ($b$) min. The frame size is $220 \times 280\,\mu$m.

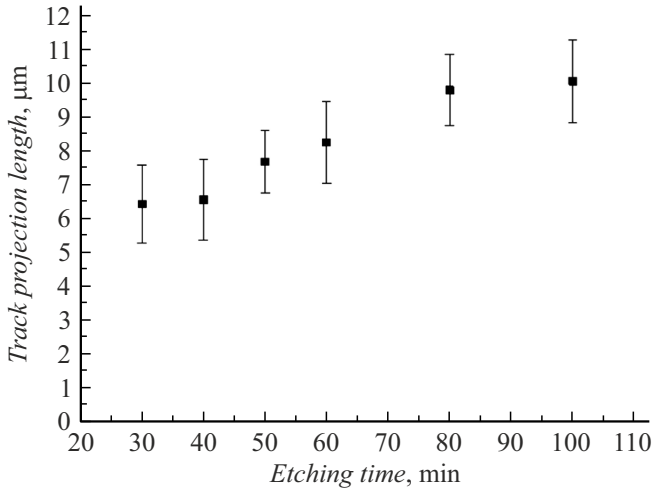



**Figure 10.** Dependence of the projection length of tracks of Xe ions with an energy of 83 MeV on the surface of the Ms mica sample on the etching time.

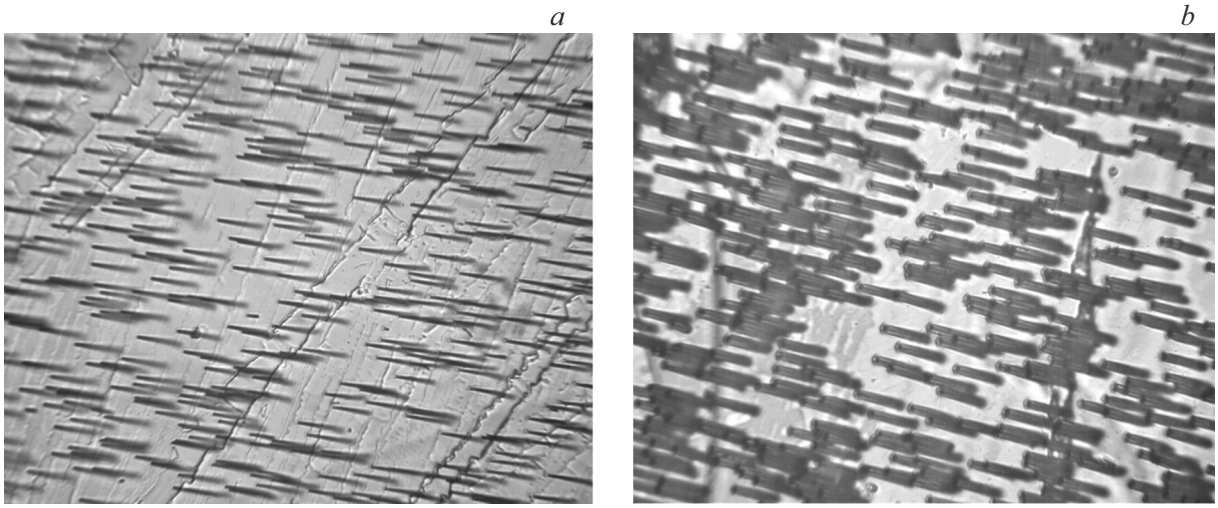



**Figure 11.** Photos of tracks of the Bi ions with an energy of 670 MeV in the Ms mica samples after etching in 40 % HF. The etching time is 20 ($a$) and 70 ($b$) min. The frame size is $220 \times 280\,\mu$m.

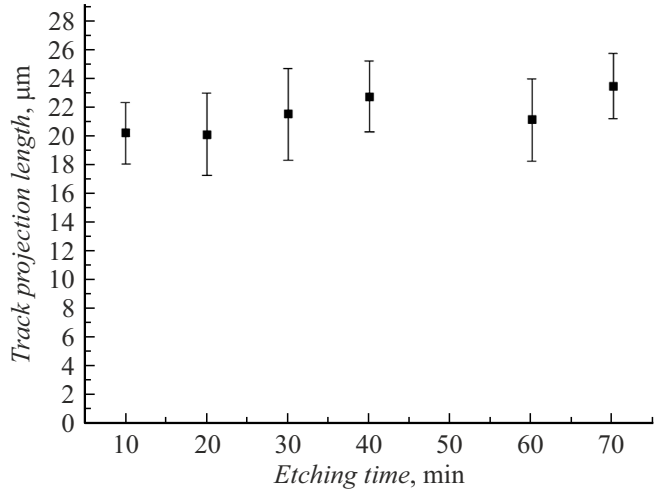



**Figure 12.** The length of the projection of tracks of the Bi ions with an energy of 670 MeV in the Ms mica samples as a function of the etching time.

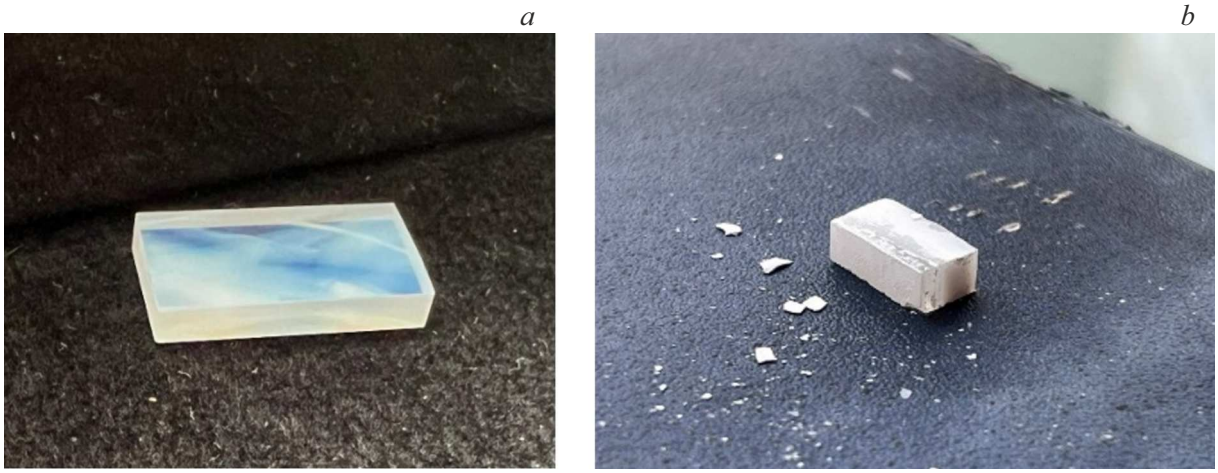



**Figure 13.** Sample of fluorophlogopite of the grade SM-310 before etching ($a$), after etching ($b$) in fluoric acid for 30 min. The sample size is $3 \times 5 \times 10$ mm.

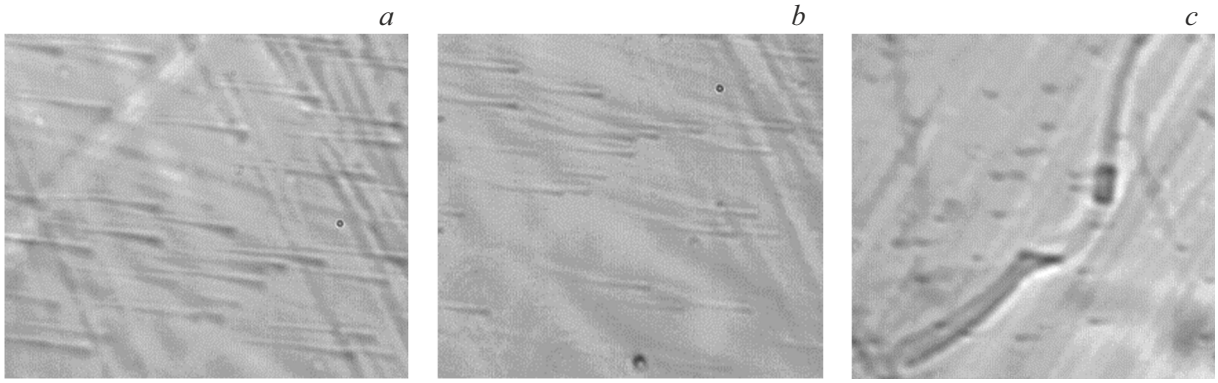



**Figure 14.** Photos of tracks of the Bi ions with an energy of 670 MeV: *a* — falling on the surface of the Ms mica sample annealed for 10 min at the temperature of 300 °C; *b* — at the depth of 5 $\mu$m from this surface; *c* — exiting a back side of the sample with an energy of 45 MeV. The size of the view field is 66 × 58 $\mu$m.

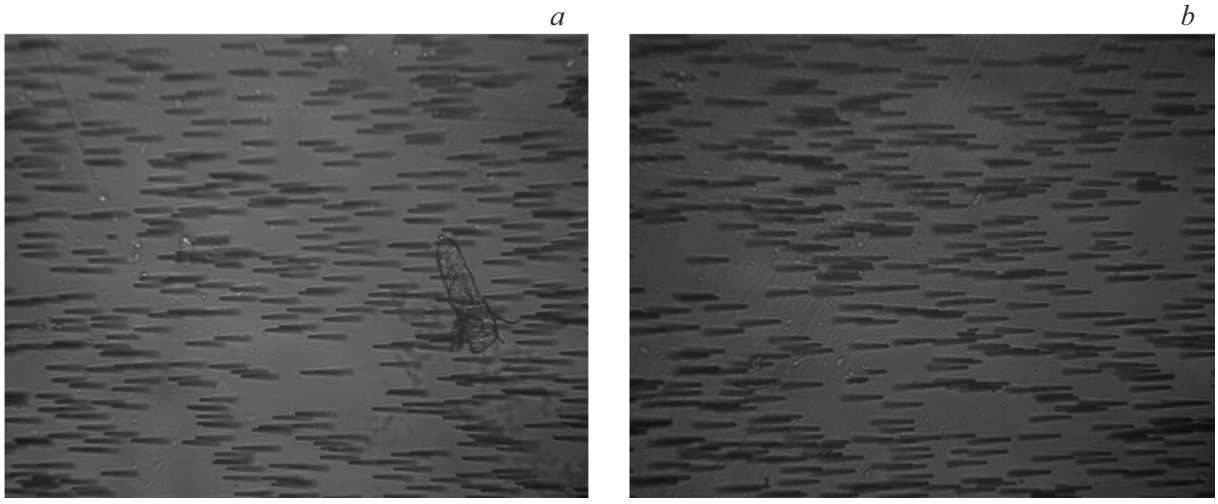



**Figure 15.** Fragments of the surface of Ms-Lpd mica samples irradiated with Bi ions with an energy of 670 MeV and etched in 40 % HF for 25 min. Before etching, the samples were annealed at 500 °C for 10 min (*a*) and 3 h (*b*). The frame size is 220 × 280 $\mu$m, magnification is 40×.

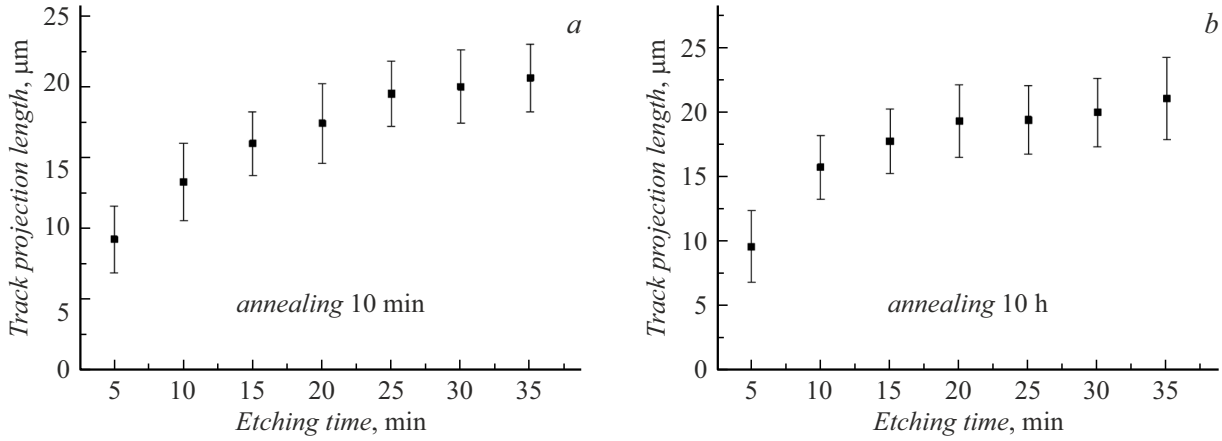



**Figure 16.** Dependence of the track projection length on the etching time in the Ms-Lpd mica samples. The annealing time at the temperature of 500 °C 10 min (*a*) and 3 h (*b*).

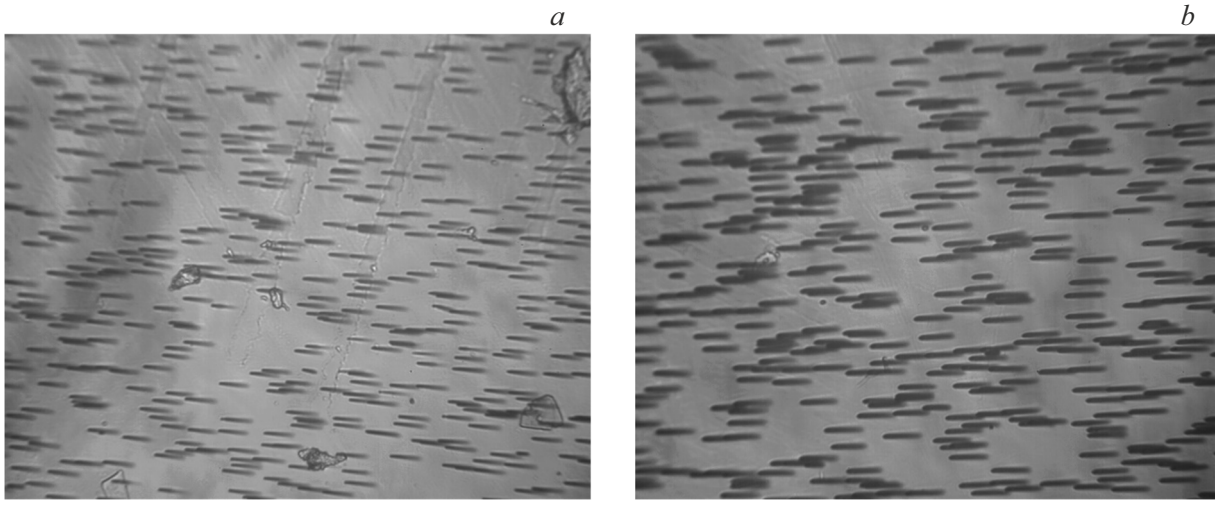



**Figure 17.** Photos of the tracks of Bi ions with an energy of 670 MeV etched with 40 % HF in the Ms-In mica samples heated after irradiation up to 500 °C and exposed at this temperature for 3 h. The annealing time is 20 (*a*) and 40 (*b*) min. The frame size is $220 \times 280\,\mu$m.

value of the path length of a Bi ion with an energy of 670 MeV in this material makes 32.3 $\mu$m.

The etching rate of the mineral in the track area at annealing for 10 min is $(67 \pm 2)\,\mu$m/h, and it makes $(81 \pm 2)\,\mu$m/h when annealing for 3 h. Thus, annealing of Ms-Lpd mica samples at a temperature of 500 °C did not result in significant variation of the track length.

Some samples of the Ms-In mica, irradiated at the angle of 45° with Bi ions with an energy of 670 MeV, after irradiation were also annealed at 500 °C with exposure at this temperature for 3 h. The images of the tracks obtained as a result of etching the annealed samples are shown in Fig. 17. Fig. 18 shows the experimental dependence of the track projection length onto the surface of the annealed sample on the etching time. The inflection, as shown in Fig. 18, occurs after etching for 30 min. The track projection length in this point is $(19 \pm 1)\,\mu$m, the path length is Fx57xEm (an estimated path length is 32.3 $\mu$m), and the track etching rate is $(55 \pm 1)\,\mu$m/h. Thus, ten-hour annealing of the samples of „Indian muscovite“ Ms-In at the temperature of 500 °C results in slight track shortening, but a noticeable increase of their etching rate.

In conclusion, Fig. 19 shows the dependence of the etching rate in the track area on charge and energy for Xe (83 and 160 MeV) and Bi (670 MeV) ions. The data are obtained for the micas Ms-Lpd and Ms-In.

As follows from Fig. 19, the micas Ms-Lpd and Ms-In exhibit a strong dependence of the etching rate in the track area on the ion charge and energy. The pronounced dependence of the ion path on its characteristics makes it possible to develop a method for determining the charge and energy of the ion by the etching rate and path before stopping in the detector material.

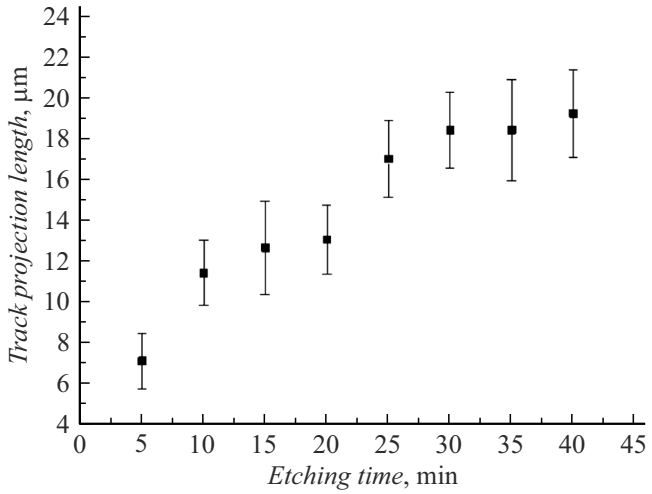



**Figure 18.** Dependence of the projection length of tracks of Bi ions with an energy of 670 MeV on the surface of the annealed mica sample Ms-In on the etching time.

## Conclusion

Study of various materials as accelerated heavy ion detectors for the JINR Factory of Superheavy Elements is going on. The paper presents the results of studies of four micas iirradiated with Xe and Bi ions with energies from 83 to 670 MeV. To simulate the experimental conditions for registration fragments of superheavy nuclei in a thermochromatographic column, some of the irradiated samples were heated to the temperatures 300 °C and 500 °C.

The analysis held showed that of the tested micas muscovite-lepidolite Ms-Lpd and „Indian“ muscoviteMs-In can be considered as ion detectors under high-temperature

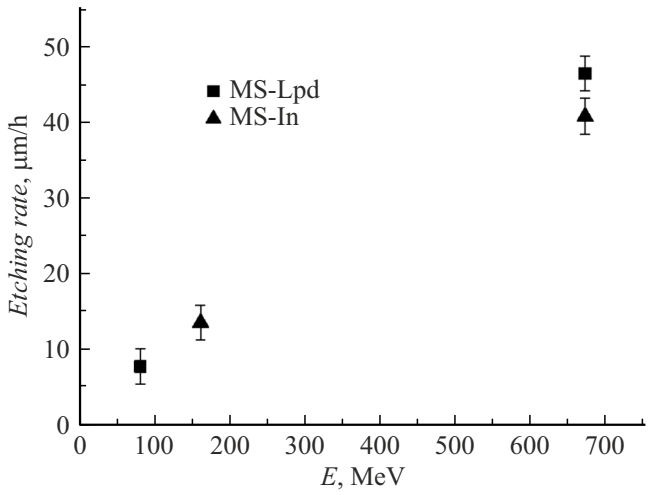



**Figure 19.** Dependence of the etching rate in the track area on charge and energy for Xe (83 and 160 MeV) and Bi (670 MeV) ions. The data are obtained for the micas Ms-Lpd and Ms-In. Ms-Lpd and Ms-In.

conditions. Presumably, this result can be conditioned by specific features of the mineral structures.

### Funding

The study was supported by the Russian Science Foundation under the program „Conducing fundamental scientific research and exploratory scientific research by individual scientific groups“ (project №. 23-12-00054). The chemical composition of the micas was studied as part of the RAS R&D topic № FMUF-2022-0002.

### Conflict of interest

The authors declare that they have no conflict of interest.

## References

[1] T.S. Zvarova, I. Zvara. *Razdelenie transuranovykh elementov pri pomoshchi gazovoi khromatografii khloridov* (R6-4911, OIYaI, Dubna, 1970) (in Russian).
[2] B.L. Zhuikov. *Metody razdeleniya letuchikh elementov i oksidov v poiske sverhtyazhelykh elementov i pri poluchenii radioizotopov* (Avtoref. kand. diss., MGU, M., 1982) (in Russian).
[3] N. Burtebayev, M. Chernyavskiy, A. Gippius, G. Kalinina, N. Konovalova, M. Nassurlla, T. Kvochkina, M. Nassurlla, N. Okateva, A. Pan, N. Polukhina, Z. Sadykov, T. Shchedrina, N. Starkov, E. Starkova, I. Zasavitskii. Universe, **8** (9), ID 474 (2022). DOI: 10.3390/universe8090474
[4] N. Burtebaev, K. Argynova, M.M. Chernyavskiy, A.A. Gippius, N.S. Konovalova, T.N. Kvochkina, M. Nasurlla, N.M. Okateva, A.N. Pan, N.G. Polukhina, Zh.T. Sadykov, T.V. Shchedrina, N.I. Starkov, E.N. Starkova, I.I. Zasavitsky. J. Exp. Theor. Phys., **134**, 528 (2022). DOI: 10.1134/S1063776122040033
[5] N. Burtebayeva, K. Argynova, M.M. Chernyavskiy, A.A. Gippius, G.V. Kalinina, N.S. Konovalova, M. Nassurlla, N.M. Okateva, A. Pan, N.G. Polukhina, Zh.T. Sadykov, T.V. Shchedrina, N.I. Starkov, E.N. Starkova, I.I. Zasavitskii. Bull. Lebedev Phys. Inst., **50** (4), 133 (2023). DOI: 10.3103/S106833562304005X
[6] P.Yu. Apel, M.M. Chernyavskiy, A.A. Gippius, G.V. Kalinina, N.S. Konovalova, N.M. Okateva, N.G. Polukhina, Zh.T. Sadykov, T.V. Shchedrina, N.I. Starkov, E.N. Starkova, I.I. Zasavitskii. Bull. Lebedev Phys. Inst., **51** (4), 117 (2024). DOI: 10.3103/S1068335624600062
[7] E. Andreev, P. Apel, N. Konovalova, N. Okateva, N. Polukhina, G. Sadykov, N. Starkov, E. Starkova, D. Strekalina, M. Chernyavskiy, T. Shchedrina. Tech. Phys., **70** (1), 174 (2025). DOI: 10.61011/TP.2025.01.60524.272-24
[8] A. Kapustsik, V.P. Perelygin, V.I. Sviderskii, S.P. Tret'yakova. *Primenenie slyudy i kvartsevogo stekla dlya registratsii deleniya yader pri povyshennykh temperaturakh* (R-2705, OIYaI, Dubna, 1966) (in Russian).
[9] S.A. Durrani, R.K. Bull. *Solid state nuclear track detection: Principles, methods and applications* (Pergamon Press, Oxford, NY., 1987)
[10] S.R. Hashemi-Nezhad. Nucl. Instrum. Methods Phys. Res. B, **234** (4), 533 (2005). DOI: 10.1016/j.nimb.2005.02.021
[11] M. Singh, N. Kaur, L. Singh. Radiat. Phys. Chem., **79** (12), 1180 (2010). DOI: 10.1016/j.radphyschem.2010.07.014
[12] M. Deb, S.C. Sarkar. In: *Minerals and Allied Natural Resources and their Sustainable Development.* (Springer Geology, Singapore, 2017), DOI: 10.1007/978-981-10-4564-6_4
[13] N.V. Vasil'ev, O.V. Udoratina, N.B. Skorobogatova, G.P. Borodulin. Vestnik IMin UrO RAN, **1** (205), 009 (2012). https://sciup.org/149129048 (in Russian).
[14] J.F. Ziegler, M.D. Ziegler, J.P. Biersack. Nucl. Instrum. Methods Phys. Res. B, **268** (11–12), 1818 (2010). DOI: 10.1016/j.nimb.2010.02.091
[15] V.T. Vasilev, N.S. Konovalova, N.M. Okatieva, N.G. Polukhina, Zh.T. Sadykov, E.N. Starkova, N.I. Starkov, M.M. Chernyavskiy, T.V. Shchedrina. Phys. Atom. Nucl., **86**, 2251 (2023). DOI: 10.1134/S1063778823090272
[16] N. Burtebayev, K. Argynova, M.M. Chernyavskiy, A.A. Gippius, G.V. Kalinina, N.S. Konovalova, T.N. Kvochkina, M. Nassurlla, N.M. Okateva, A. Pan, N.G. Polukhina, Zh.T. Sadykov, T.V. Shchedrina, N.I. Starkov, E.N. Starkova, I.I. Zasavitskii. Bull. Lebedev Phys. Inst., **49** (10), 350 (2022). DOI: 10.3103/S1068335622100062
[17] S.P. Tret'yakova. EChAYa, **23** (2), 364, 1992. (in Russian).
[18] V.A. Nikolaev. *Tverdotel'nye trekovye detektory v radiatsionnykh issledovaniyakh* (Izd-vo Politekh. un-ta, SPb, 2012) (in Russian).

*Translated by M.Shevelev*